Catalysis Letters (2019) 149:449–455
https://doi.org/10.1007/s10562-018-2625-8

Benzyl Alcohol Oxidation Using Gold Catalysts Derived from Au_8 Clusters on TiO_2

Rohul H. Adnan[1] · **Vladimir B. Golovko**[2]

Received: 8 September 2018 / Accepted: 27 November 2018 / Published online: 4 December 2018

Abstract

Atomically-precise gold clusters have gained attraction in catalysis due to high fraction of low-coordinated gold atoms, unique structural geometry and ligand effect. Phosphine-ligated gold clusters offer an advantage in the light of the labile gold-phosphorous bond for easy ligand removal. Here, heterogeneous gold catalysts were prepared by depositing atomically-precise phosphine-ligated gold clusters, $Au_8(PPh_3)_8(NO_3)_2$ onto anatase-phase TiO_2 nanoparticles. The catalysts were then calcined under two different conditions: O_2 (Au_8/TiO_2:O_2) and O_2 followed by H_2 (Au_8/TiO_2:O_2–H_2) at 200 °C, to dislodge phosphine ligands from the Au core. It was found that Au_8/TiO_2:O_2–H_2 catalyst showed a decent catalytic activity in benzyl alcohol oxidation while Au_8/TiO_2 and Au_8/TiO_2:O_2 were completely inactive. Such results imply that small-size gold clusters (2–3 nm) alone do not always contribute to high catalytic activity of gold catalysts. It is suggested that the presence of NO_3^- species defines the catalytic activity of supported gold clusters in benzyl alcohol oxidation in the case of these catalysts and reinforces our initial claim in the previous work.

Electronic supplementary material The online version of this article (https://doi.org/10.1007/s10562-018-2625-8) contains supplementary material, which is available to authorized users.

✉ Rohul H. Adnan
rohuladnan@gmail.com; rohulhayat@utm.my

[1] Department of Chemistry, Faculty of Science, Universiti Teknologi Malaysia, 81310 Johor Bahru, Malaysia

[2] School of Physical and Chemical Sciences, University of Canterbury, Private Bag 4800, Christchurch 8140, New Zealand

Graphical Abstract

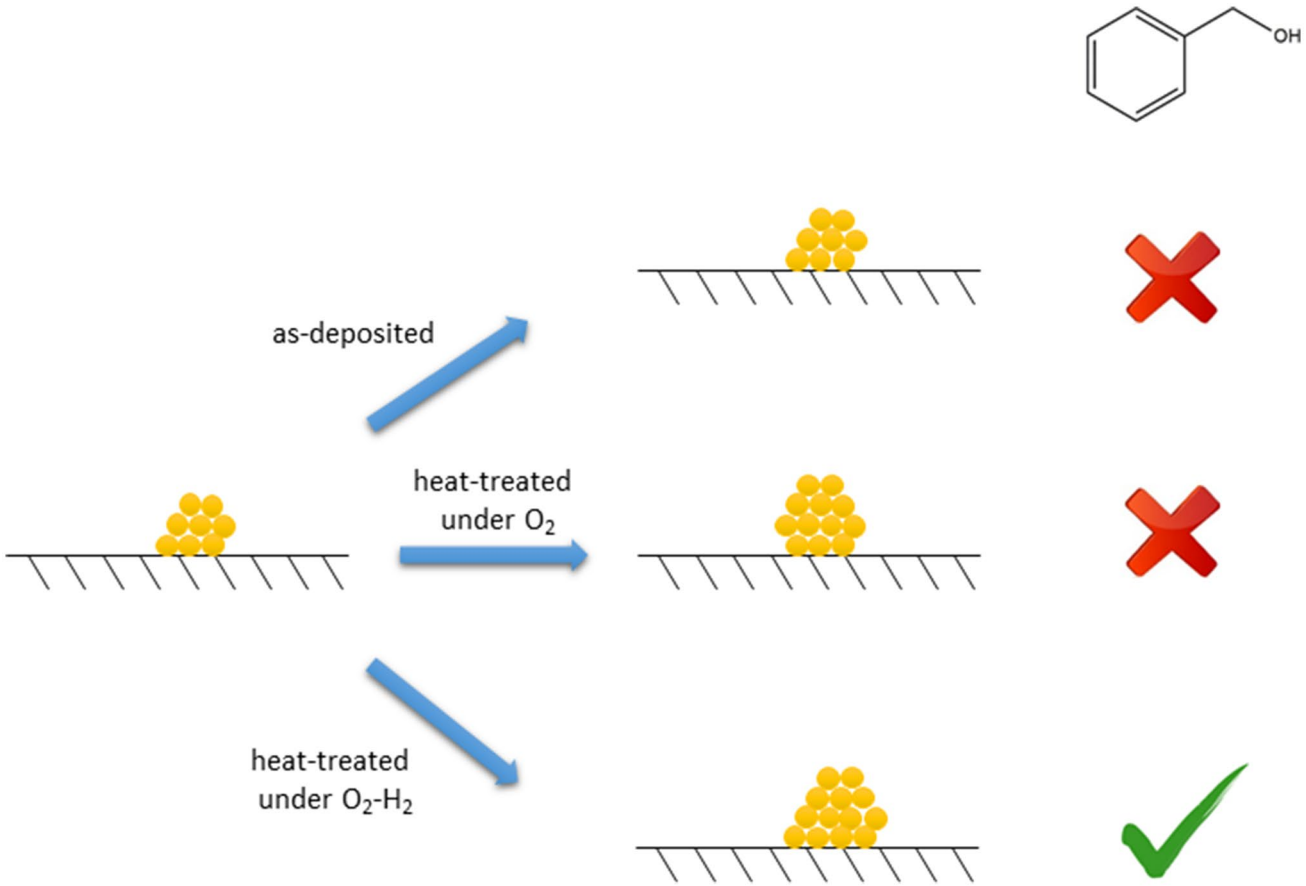

Keywords Heterogeneous catalysis · Alcohols · Oxidation · Green chemistry

1 Introduction

The discovery of catalytic activity of small gold particles on metal oxides in CO oxidation 1987 by Haruta et al. has triggered a gold rush in catalysis [1] Since then, numerous works on catalytic activity of gold nanoparticles, both supported and unsupported, have been reported in the literature [2–6]. More importantly, the catalytic activity of gold nanoparticles have been extended into a range of chemical reactions such as hydrogenation of alkenes, aldehydes and ketones, reduction of nitro compounds and photodegradation of pollutants [7–14].

Recently a class of atomically precise gold clusters gained attention because of their high yield synthesis, low coordination number of gold atoms and well-defined crystallographic structure [15, 16]. Phosphine-ligated gold clusters are preferred over thiolate gold analogues because of facile removal of phosphine ligands due to the labile Au-P bond and the absence of catalytic poisoning sulphur-containing ligands. For example, Golovko et al. have reported the use of phosphine-stabilized gold clusters on metal oxides in cyclohexene and benzyl alcohol oxidation [17–19].

Despite promising catalytic activity of gold clusters and nanoparticles, the genesis of their catalytic activity and the nature of the active sites are still under debate. Haruta highlighted that three major factors define the catalyst performance of gold catalysts: contact structure at the interface between gold nanoparticles and the support, type of supports and gold particle size [20]. Hutchings and co-workers determined that the active gold clusters on iron oxide for CO oxidation is attributed to bilayer clusters that contain only ~ 10 gold atoms while monolayer clusters containing 3–4 gold atoms appear inactive [21]. Yoon et al. revealed that charging of Au_8 clusters resulting from the partial transfer of charge from the MgO support is responsible for the catalytic activity in CO oxidation [22]. Zhu et al. and Liu et al. observed that the catalytic activity increased as the gold cluster size decreased in oxidation of styrene and benzyl

alcohol, respectively [23–25]. In contrast, Haider et al. reported that small size Au particle was not necessary for high catalytic activity in benzyl alcohol oxidation and found that the catalyst with medium particle size (6.9 nm) showed the highest activity as compared to the smaller-sized catalysts irrespective of the supports [26]. Interestingly, Donoeva et al. observed that the catalytic activity of gold clusters only appeared after larger particles (> 2 nm) had formed while the smaller ones (< 2 nm) were inactive in cyclohexene oxidation [17].

Besides size effect, other factors such as ligand and counter ions effects have been investigated. A recent work by Wan et al. investigated the ligand effect of gold clusters on hydrogenation of alkynes using the Au_{38} gold clusters [27]. Despite similar, sub-2 nm size Au clusters (~ 1.4 nm), alkynyl-ligated Au clusters displayed superior catalytic activity (conversion > 97%) than thiolate-ligated ones (< 2%). Yuan et al. prepared gold catalysts from gold-phosphine complexes containing nitrate (NO_3^-) counter ions for CO oxidation [28]. The catalyst only showed decent activity after heat-treatment under CO_2 and H_2/Ar atmosphere, which may cause decomposition of NO_3^- species. Contrary to work of Yuan et al., Solsona et al. reported that NO_3^- anions had a beneficial effect that promoted catalytic activity for CO oxidation when the anions were added by impregnation method and without heat treatment [29]. Adnan et al. reported the effect of counter ions (NO_3^- and Cl^-) in phosphine-ligated gold clusters (Au_9 and Au_{101}) supported on TiO_2 and SiO_2 in benzyl alcohol oxidation [19]. The authors observed a distinct effect of counter anions present in the gold clusters with NO_3^- diminished the catalytic activity of gold catalysts. It is clear that different, incoherent findings from different groups of authors/researchers lead to lack of agreement about the nature of the active site of gold catalyst.

Herein, we reported the catalytic activity of another type of phosphine-stabilized gold cluster, $Au_8(PPh_3)_8(NO_3)_2$ (referred to as Au_8) in benzyl alcohol oxidation. The aim of this work is to study the effect of post deposition heat treatment (post-treatment) conditions on the catalytic performance of Au_8 cluster-derived catalysts in benzyl alcohol oxidation. Three different materials were produced: as-deposited without any post-treatment (Au_8/TiO_2), and post-treated—calcined under O_2 (Au_8/TiO_2:O_2) and calcined under O_2 followed by H_2 (Au_8/TiO_2:O_2–H_2). It was found that the most active catalyst was Au_8/TiO_2:O_2–H_2 while the former two were completely inactive.

2 Experimental

Au_8 clusters were prepared according to the published synthetic method elsewhere [30, 31]. The yield of Au_8 clusters produced was 180 mg (85%). Elemental analysis gave the result: %C: 45.7 (45.5), %H: 3.27 (3.16) and %N: 0.81 (0.74) with the calculated values in parentheses. Thermogravimetric analysis (TGA) of pure microcrystalline Au_8 (Fig. S1 in ESI) onset of the ligand loss at 239 °C, with overall loss of 60% corresponding to loss of ligands and nitrate counter ions and residual *ca*. 40% correlating with calculated 41.5 wt% of gold. Deposition of Au clusters onto TiO_2 nanopowders (SkySpring Nanomaterials, 99.5%, 10–30 nm particle size, *ca*. 70 m^2/g) was reported in our previous works [19, 32]. Calcination was performed using Schlenk line techniques under pure O_2 atmosphere at 200 °C for 2 h (labelled as Au_8/TiO_2:O_2) and under pure O_2 followed by H_2 atmosphere at 200 °C for 2 h (labelled as Au_8/TiO_2:O_2–H_2). All catalysts were stored in the fridge at 4 °C fur further use and characterization.

High-resolution bright field transmission electron microscopy (HRTEM) imaging was performed using a Philips CM200 TEM operating at 200 kV. TEM samples were prepared by drop-casting two drops of catalyst suspension (0.1 mg/mL in methanol) onto Cu (300 mesh) grids coated with a holey carbon film. UV–Vis diffuse reflectance spectroscopy (UV–Vis DRS) spectra were recorded using a Cintra 404 (GBC Scientific Equipment) spectrophotometer.

Catalytic testing was performed according to our previous publication [19]. Typically, a mixture of benzyl alcohol (0.270 g, 2.50 mmol), anisole (0.135 g, 1.25 mmol) as internal standard and methanol (25 mL) as solvent were charged into a Teflon liner. Then, K_2CO_3 (0.345 g, 2.50 mmol) and catalyst (50 mg) were added. The autoclave was pressurised with 5 bar of oxygen and heated to 80 °C for 4 h. Each catalytic test was repeated at least in triplicate giving lower than 5% differences in conversion and selectivity. Product mixtures were identified and quantified using a high-performance liquid chromatography (HPLC) Dionex Ultimate 300 system and eluted with a mixture of 0.05 v/v% trifluoroacetic acid in water (70%) and acetonitrile (30%).

3 Results and Discussion

Representative TEM images of Au_8 clusters on TiO_2 are shown in Fig. 1a–c; the cirlces indicate the gold clusters on TiO_2 supports. For the as-deposited Au_8/TiO_2 sample, majority of gold clusters exist as small clusters or minimally aggregated clusters aroud 1.2 nm. Due to the resolution limit of the conventional HRTEM (Philips CM200 TEM) and poor contrast of these clusters over support material, imaging such small clusters is very challenging [17]. Additionally, the low gold loading (0.17 wt%) adds difficulty in imaging such small clusters and constructing a statistical histogram, and thus we infer that the size of Au_8 clusters in the Au_8/TiO_2 sample is below 2 nm. Nonetheless, the absence of larger gold particles which are visible in TEM

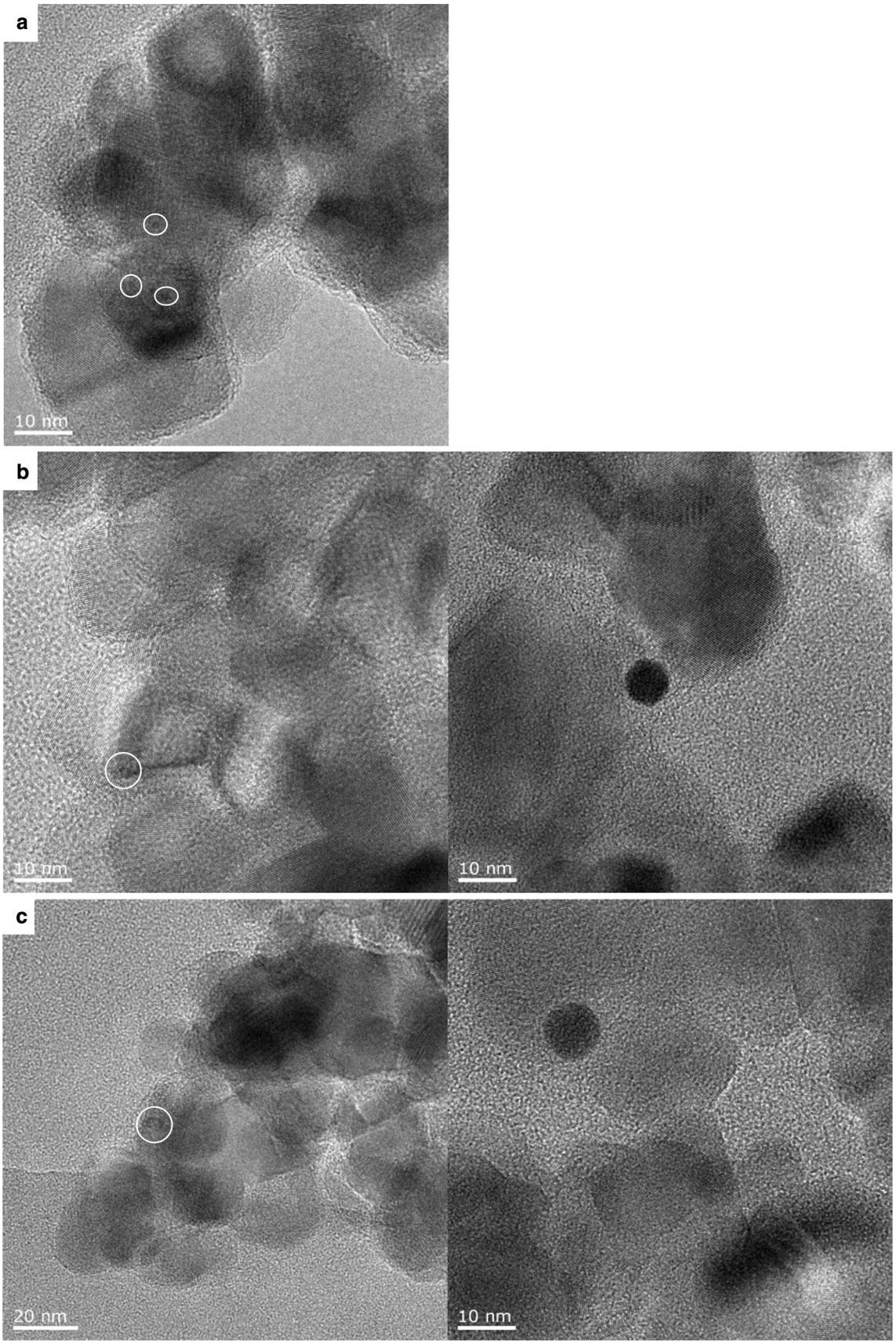

Fig. 1 Representative TEM image of **a** Au_8/TiO_2, **b** Au_8/TiO_2:O_2 and **c** Au_8/TiO_2:O_2–H_2 catalyst samples

(from imaging different areas on the Cu grid) suggests that the dominant population is small gold clusters. Upon calcination under O_2 Au_8 clusters aggregate to form larger gold particles with a mean size of 2.2 ± 1.5 nm. It is worth mentioning that the uncertainty in the mean particle size is the standard deviation of particle size distribution, not the width of particle size distribution itself. Figure 1b displays representative TEM images of Au_8/TiO_2:O_2 catalysts. It can be clearly seen the presence of small Au_8 clusters around 3 nm (Fig. 1b, left) and 8 nm (Fig. 1b, right), however 5–6 nm particles are hardly observed under TEM imaging. Further calcination under H_2 at 200 °C increased the mean particle size to 2.5 ± 1.7 nm. Representative TEM images show an Au particle with 5 nm size (Fig. 1c, left) and 10 nm size (Fig. 1c, right). A large fraction of Au particles in both calcined (under O_2 and O_2–H_2) are below 4 nm. Statistical histograms for particle size of both calcined catalysts are provided in Electronic Supplementary Information (Figs. S2, S3).

To further verify the TEM imaging results, UV–Vis DR spectra were recorded for all catalysts (Fig. 2). The as-deposited Au_8/TiO_2 sample (Fig. 2, black, bottom curve) displays a molecular-like optical properties with a few distinct peaks below 500 nm and absence of localized surface plasmon resonance (LSPR) band, characteristic of larger gold nanoparticle with metallic state [33]. The transition from non-metallic clusters to nanoparticles has been reported to occur around 2.25 nm [34]. Thus, it is sufficient and reasonable to conclude that gold clusters in the as-deposited Au_8/TiO_2 catalysts have a dominant population with size below 2.25 nm. Similarly, Al Qahtani et al. also reported that as-deposited Au_9 clusters on TiO_2 nanosheets were predominantly unaggregated clusters and some minimally aggregated clusters with particle size below 2.25 nm [35]. Spectra of both

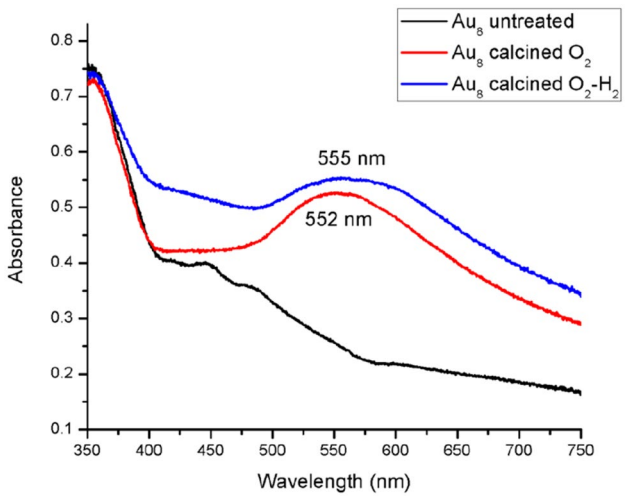

Fig. 2 UV–Vis DR spectra of the Au_8/TiO_2 based catalysts

heat-treated Au_8 catalysts show loss of peaks associated with gold-phosphine clusters, comfirming ligand removal from the cluster cores. Yet, both heat-treated Au_8 catalysts displayed the presence of LSPR bands at 552 nm (for Au_8/TiO_2:O_2) and 555 nm (for Au_8/TiO_2:O_2–H_2) respectively, which indicated that there are larger, metallic gold particles present in such samples with particle sizes larger than 2.25 nm. The red-shift of the LSPR band in the UV–Vis DR spectrum from Au_8/TiO_2:O_2 to Au_8/TiO_2:O_2–H_2 catalysts revealed there was an increase in the gold particle size [36], consistent with the finding from HRTEM imaging. While the LSPR red-shift is indicative of an increase the gold particle size, the position of the LPSR peak maximum cannot be used to estimate the particle size because it depends on a number of factors: size, shape/morphology, stabilizing ligands, composition (core–shell structure, doping), solvent and dielectric constant of surrounding medium e.g. support [37–39]. A significant example is the position of LSPR peak maximum for thiolated-protected Au clusters reported by Zhou et al. [40]. The LSPR peak for Au_{333}, $Au_{\sim 520}$ and $Au_{\sim 940}$ clusters are 540, 525 and 525 nm, respectively. The broad LSPR peak for both calcined Au_8 catalysts reflects the broad size distribution which is consistent with the finding from TEM imaging.

XPS studies on as-deposited Au_8 clusters on TiO_2 revealed that some phosphine ligands already dislodged from the gold core exposing the active site to the substrate [32]. Hence, the argument that steric phosphine ligands block the active site does not apply in this case. Presence of both clusters and larger, bulk-like gold particles can be monitored by XPS [41, 42]. Our earlier XPS study (see Figs. 1A, 2, and Table 1 in [32]) revealed presence of clusters and bulk-like gold particles, with characteristic Au $4f_{7/2}$ peak intensity ratio of ca. 1.6 implying prevalence of clusters species, already in the "as deposited" Au_8/TiO_2 [32]. The bulk-like species in this case are likely to be closer in properties to the Au_{101}, which is non-plasmonic yet did show Au $4f_{7/2}$ binding energy of 83.9 ± 0.1. Whereas proportion of the bulk-like particles significantly increased upon calcination under O_2 (Au$4f_{7/2}$ peak intensity ratio diminished to *ca*. 0.9, implying majority of bulk-like Au species). After combined O_2-H_2 treatment (twice as long at high temperature cf. O_2 treatment alone) we were unable to detect characteristic signature of gold clusters (< 2 nm).

The catalytic activity of the catalysts was tested in benzyl alcohol oxidation (summarized in Table 1). The as deposited clusters, Au_8/TiO_2 catalyst, was completely inactive despite having a particle size below 2 nm. This finding is in contrast with reports that found the ultra-small clusters (< 2 nm) should possess high catalytic activity in benzyl alcohol oxidation albeit the reaction condition was different (the use of microwave heating and H_2O_2 as oxidant) [24, 43]. The Au_8/TiO_2:O_2 catalyst also did not show any catalytic

Table 1 Conversion and selectivity in benzyl alcohol oxidation using Au_8 on TiO_2 catalysts

Au_x/TiO_2 catalysts	Conversion (%)	Selectivity (%)		Refs.
		Methyl benzoate	Benzoic acid	
Au_8 as-deposited	0	0	0	This work
Au_8 calcined O_2	0	0	0	This work
Au_8 calcined O_2–H_2	30	37	48	This work
Au_9 as-deposited[a]	0	0	0	[19]
Au_9 calcined O_2[a]	0	0	0	[19]
Au_9 calcined O_2–H_2[a]	20	23	18	[19]
Au_{101} as-deposited[b]	0	0	0	[19]
Au_{101} calcined O_2[b]	96	79	21	[19]
Au_{101} calcined O_2–H_2[b]	97	75	23	[19]

Reaction condition: benzyl alcohol (0.270 g, 2.50 mmol), anisole (0.135 g, 1.25 mmol) as internal standard, methanol (25 mL), K_2CO_3 (0.345 g, 2.50 mmol) and catalyst (50 mg) reacted at 5 bar of O_2 at 80 °C for 4 h

[a]The molecular formula is $Au_9(PPh_3)_8(NO_3)_3$

[b]The average formula is $Au_{101}(PPh_3)_{21}Cl_5$

activity after an increase in the particle size and the presence of metallic state (through the appearance of LSPR band). However, the Au_8/TiO_2:O_2–H_2 catalyst showed a discernible, significant catalytic activity at 30% benzyl alcohol conversion to methyl benzoate and benzoic acid.

Considering that the mean particle size and the position of the LSPR band are very similar for Au_8/TiO_2:O_2 and Au_8/TiO_2:O_2–H_2 catalysts, we reason that the heat treatment under H_2 atmosphere changed the nature of the Au cluster catalysts. Our earlier XPS study failed to detect the presence of N 1*s* peaks due to the ultra-low loading of Au clusters (0.17 wt%) on TiO_2 leading to unclear fate of NO_3^- anions after heat treatment. However, decomposition of NO_3^- anions under the H_2 stream into N_2 and N_2O gases was reported by Hirayama and Kamiya [44]. Our earlier work employing two different gold clusters, $Au_{101}(PPh_3)_{21}Cl_5$ (referred to as Au_{101}) and $Au_9(PPh_3)_8(NO_3)$ (referred to as Au_9) exhibited a distinct catalytic activity with Au_9 containing NO_3^- anions was catalytically inactive [19]. The similar trend of catalytic activity of Au_8 and Au_9 clusters, which are derived from $Au_8(PPh_3)_8(NO_3)_2$ and $Au_9(PPh_3)_8(NO_3)_3$, respectively, reinforces our initial suggestion that the presence of NO_3^- inhibits the catalytic activity of gold clusters in benzyl alcohol oxidation.

The catalytic activity of Au clusters cannot be attributed solely to the gold particle size. Haruta suggested that at least three main factors are involved in defining catalytic performance of gold catalysts: size of gold particles, contact structure of gold-support perimeter interface and type of supports [45]. Very recently Wan et al. reported that stabilizing ligands play a crucial role in defining the catalytic activity of Au_{38} clusters for hydrogenation of alkynes [27]. We believe that complex contributing factors govern the catalytic performance of gold clusters and further works are under way to investigate these factors.

4 Conclusion

In summary, we have observed that Au_8/TiO_2 and Au_8/TiO_2:O_2 catalysts were inactive in benzyl alcohol oxidation. Meanwhile a significant increase in benzyl alcohol conversion by 30% was observed for Au_8/TiO_2:O_2–H_2 catalysts suggesting that the heat treatment under the H_2 stream changed the nature of the NO_3^- species present in the gold clusters. NO_3^- anions were suggested to inhibit the catalytic activity of gold clusters in benzyl alcohol oxidation.

Acknowledgements The authors would like to thank Professor Milo Kral and Mike Flaws for their help with HRTEM imaging, Dr. Meike Holzenkaempfer and Dr. Marie Squire for development of the HPLC methodology. This work was supported by the MacDiarmid Institute for Advanced Materials and Nanotechnology, University of Canterbury.

References

1. Haruta M, Kobayashi T, Sano H, Yamada N (1987) Chem Lett 16:405–408
2. Haruta M, Yamada N, Kobayashi T, Iijima S (1989) J Catal 115:301–309
3. Yuan Y, Asakura K, Wan H, Tsai K, Iwasawa Y (1996) Chem Lett 25:755–756
4. Prati L, Rossi M (1998) J Catal 176:552–560
5. Iizuka Y, Tode T, Takao T, Yatsu K-i, Takeuchi T, Tsubota S, Haruta M (1999) J Catal 187:50–58
6. Porta F, Prati L, Rossi M, Coluccia S, Martra G (2000) Catal Today 61:165–172
7. Bond GC, Sermon PA (1973) Gold Bulletin 6:102–105
8. Bailie JE, Hutchings GJ (1999) Chem Commun 21:2151–2152
9. Milone C, Ingoglia R, Schipilliti L, Crisafulli C, Neri G, Galvagno S (2005) J Catal 236:80–90
10. Milone C, Tropeano ML, Gulino G, Neri G, Ingoglia R, Galvagno S (2002) Chem Commun 8:868–869
11. Li G, Zeng C, Jin R (2014) J Am Chem Soc 136:3673–3679
12. Tamiolakis I, Fountoulaki S, Vordos N, Lykakis IN, Armatas GS (2013) J Mater Chem A 1:14311–14319
13. Pritchard J, Kesavan L, Piccinini M, He Q, Tiruvalam R, Dimitratos N, Lopez-Sanchez JA, Carley AF, Edwards JK, Kiely CJ, Hutchings GJ (2010) Langmuir 26:16568–16577
14. Corma A, Serna P (2006) Science 313:332–334
15. Negishi Y, Nakazaki T, Malola S, Takano S, Niihori Y, Kurashige W, Yamazoe S, Tsukuda T, Häkkinen H (2015) J Am Chem Soc 137:1206–1212
16. Gutrath BS, Englert U, Wang Y, Simon U (2013) Eur J Inorg Chem 2013:2002–2006
17. Donoeva BG, Ovoshchnikov DS, Golovko VB (2013) ACS Catal 3:2986–2991
18. Ovoshchnikov DS, Donoeva BG, Williamson BE, Golovko VB (2014) Catal Sci Technol 4:752–757

19. Adnan RH, Andersson GG, Polson MIJ, Metha GF, Golovko VB (2015) Catal Sci Technol 5:1323–1333
20. Haruta M (2003) Chem Rec 3:75–87
21. Herzing AA, Kiely CJ, Carley AF, Landon P, Hutchings GJ (2008) Science 321:1331–1335
22. Yoon B, Häkkinen H, Landman U, Wörz AS, Antonietti J-M, Abbet S, Judai K, Heiz U (2005) Science 307:403–407
23. Zhu Y, Qian H, Jin R (2010) Chemistry A 16:11455–11462
24. Liu Y, Tsunoyama H, Akita T, Tsukuda T (2010) Chem Lett 39:159–161
25. Tsunoyama H, Liu Y, Akita T, Ichikuni N, Sakurai H, Xie S, Tsukuda T (2011) Catal Surv Asia 15:230–239
26. Haider P, Kimmerle B, Krumeich F, Kleist W, Grunwaldt J-D, Baiker A (2008) Catal Lett 125:169–176
27. Wan X-K, Wang J-Q, Nan Z-A, Wang Q-M (2017) Sci Adv 3:e1701823
28. Yuan Y, Asakura K, Wan H, Tsai K, Iwasawa Y (1996) Catal Lett 42:15–20
29. Solsona B, Conte M, Cong Y, Carley A, Hutchings G (2005) Chem Commun 18:2351–2353
30. Van der Velden JWA, Bour JJ, Bosman WP, Noordik JH (1983) Inorg Chem 22:1913–1918
31. Gutrath BS, Schiefer F, Homberger M, Englert U, Şerb M-D, Bettray W, Beljakov I, Meded V, Wenzel W, Simon U (2016) Eur J Inorg Chem 2016:975–981
32. Anderson DP, Adnan RH, Alvino JF, Shipper O, Donoeva B, Ruzicka J-Y, Al Qahtani H, Harris HH, Cowie B, Aitken JB, Golovko VB, Metha GF, Andersson GG (2013) Phys Chem Chem Phys 15:14806–14813
33. Gutrath BS, Schiefer F, Homberger M, Englert U, Şerb MD, Bettray W, Beljakov I, Meded V, Wenzel W, Simon U (2016) Eur J Inorg Chem 2016:975–981
34. Higaki T, Zhou M, Lambright KJ, Kirschbaum K, Sfeir MY, Jin R (2018) J Am Chem Soc 140:5691–5695
35. Al Qahtani HS, Kimoto K, Bennett T, Alvino JF, Andersson GG, Metha GF, Golovko VB, Sasaki T, Nakayama T (2016) J Chem Phys 144:114703
36. Kimling J, Maier M, Okenve B, Kotaidis V, Ballot H, Plech A (2006) J Phys Chem B 110:15700–15707
37. S. L. and and El-Sayed MA (2003) Annu Rev Phys Chem 54:331–366
38. Link S, Wang ZL, El-Sayed MA (1999) J Phys Chem B 103:3529–3533
39. Della Gaspera E, Bersani M, Mattei G, Nguyen T-L, Mulvaney P, Martucci A (2012) Nanoscale 4:5972–5979
40. Zhou M, Zeng C, Chen Y, Zhao S, Sfeir MY, Zhu M, Jin R (2016) Nat Commun 7:13240
41. Anderson DP, Alvino JF, Gentleman A, Qahtani HA, Thomsen L, Polson MIJ, Metha GF, Golovko VB, Andersson GG (2013) Phys Chem Chem Phys 15:3917–3929
42. Ruzicka J-Y, Abu Bakar F, Hoeck C, Adnan R, McNicoll C, Kemmitt T, Cowie BC, Metha GF, Andersson GG, Golovko VB (2015) J Phys Chem C 119:24465–24474
43. Liu Y, Tsunoyama H, Akita T, Tsukuda T (2009) J Phys Chem C 113:13457–13461
44. Hirayama J, Kamiya Y (2018) Cataly Sci Technol. https://doi.org/10.1039/C8CY00730F
45. Haruta M (2002) CATTECH 6:102–115